



OPEN

A clear distinction and presence of *Acropora* aff. *divaricata* within *Acropora* cf. *solitaryensis* species complex along their biogeographic distribution in East Asia

Savanna Wenhua Chow^{1,2,3,8}, Chih-Hsun Chen^{1,2,8}, Du-Yang Tsai², Takuma Mezaki⁴, Satoshi Kubota⁵, Hernyi Justin Hsieh⁶, Shashank Keshavmurthy²✉ & Chaolun Allen Chen^{1,2,3,7}✉

In the Anthropocene, scleractinian corals face unprecedented threats from synergistic stressors, including rising seawater temperatures that surpass critical thresholds that lead to global coral reef degradation. With over 1,698 coral species in the order Scleractinia, their conservation is increasingly complex due to their morphological plasticity and the challenge of accurate species identification. The genus *Acropora*, with approximately 400 nominal species, exemplifies these challenges, as morphological traits often vary within and among species, complicating taxonomic efforts. Traditional methods based on skeletal characteristics are insufficient for delineating *Acropora* species, prompting the use of integrative approaches combining morphology, reproduction, and molecular data. In this study, we employ multi-locus phylogenetic analyses and morphometric measurements to distinguish different growth forms of *Acropora* cf. *solitaryensis* as distinct species and delineate the species range boundaries of *A.* aff. *divaricata* and *A.* cf. *solitaryensis* in East Asian coral ecosystems. We identify arborescent and intermediate morphotypes belonging to *A.* aff. *divaricata*, which is distributed from tropical reefs in southeastern Taiwan to temperate non-reefal communities in Shikoku, Japan. Conversely, the solid-plate morphotype aligns with *A.* cf. *solitaryensis* from the holotype locality at Solitary Island, Australia, found primarily in subtropical non-reefal regions in northern Taiwan and Japan. The distinct distribution patterns of *A.* aff. *divaricata* and *A.* cf. *solitaryensis* underscore the necessity for biogeographic sampling in *Acropora* taxonomy, considering the Kuroshio Current's impact on coral distributions, and a re-evaluation of poleward coral migration or expansion due to climate change. Our findings challenge the traditional taxonomy of *A.* aff. *divaricata* and *A.* cf. *solitaryensis*, revealing that they may instead encompass multiple species. This has significant implications for coral conservation strategies, as accurate species identification is crucial for understanding coral responses to environmental changes and informing conservation efforts in the face of climate change.

Keywords *Acropora*, Species complex, Coral ecosystems in East Asia, Taiwan, Japan, High-latitude, Non-reefal, Climate change

Scleractinian corals are under threat in the Anthropocene due to the synergistic effects of stressors, natural and man-made¹. As we progress into the likelihood of seawater temperatures breaching a 1.5 °C threshold² and frequent and prolonged seawater temperature anomalies below and above threshold limits for coral survival^{1,3-5}, there is increased awareness and pressure for coral and coral reef conservation worldwide⁶⁻¹². While the

¹Department of Life Science, National Taiwan Normal University, Taipei 106, Taiwan. ²Biodiversity Research Center, Academia Sinica, Taipei 115, Taiwan. ³Biodiversity Program, International Graduate Program, Academia Sinica, Taipei 115, Taiwan. ⁴Kuroshio Biological Research Institute, Nishidomari, Kochi 788-0333, Japan. ⁵Kuroshio Science Unit, Kochi University, Nankoku, Kochi, Japan. ⁶Penghu Marine Biology Research Center, Fisheries Research Institute, Penghu, Taiwan. ⁷Department of Life Science, Tunghai University, Taichung 404, Taiwan. ⁸Savanna Wenhua Chow and Chih-Hsun Chen contributed equally to this work. ✉email: coralresearchtaiwan@gmail.com; cac@gate.sinica.edu.tw

Acropora divaricata		Acropora solitariyensis	
Veron and Wallace, 1984 ²³		Veron and Wallace, 1984 ²³	
Wallace, 1999 ²²		Wallace, 1999 ²²	
References	Veron and Wallace, 1984 ²³	Veron and Wallace, 1984 ²³	Wallace, 1999 ²²
Corallium			
Branching pattern	Thick tables or bowl/bracket-shaped with central or lateral attachment, 1 m or more in height and diameter	Open caespitose-corymbose with tapering branches	A. divaricata-like branching pattern, basal branches fused into a perforated or solid plate
Branch size	Caespitose branching, distal branches 6–12 mm diameter	Branches 5–15 mm in diameter, up to 70 mm	Branches 5–15 mm in diameter, up to 45 mm
Branch arrangement	Branching pattern and colony shape varying greatly	Curving and anastomosing to form a network within the colony	Anastomosing and upwardly curving
Growth type		Determinate	Determinate
Corallites			
Axial corallites	Usually 2.3–3.0 mm diameter, with calices 0.8–1.1 mm diameter	Outer diameter 1.8–3.0 mm, inner diameter 0.7–1.1 mm	Up to 3 mm exsert, 3.4 mm diameter with calices 0.7–1.0 mm diameter
Primary septa	Two cycles up to 1/2R and 1/4R, the latter frequently incomplete	Present up to 1/R	Usually in complete cycles of 1/2R
Secondary septa		Absent or some to all present to 1/4R	Usually incomplete to absent
Radial corallites	Change in shape and size along branches, from prominent on upper branchlets extending from 45° to 90°, tubular on branch tips, passing through tubo-nariform to nariform, then rounded to sub-immersed proximally	Evenly sized and spaced on branches, nariform, with large, open calices	Tubular appressed on branchlets, becoming immersed on basal branches. Circular to nariform, diameter 1.0–1.3 mm
Primary septa	Extremely variable septal development, some corallites with only rudimentary septa, others with two well-developed cycles	Present up to 1/2R with obvious directives	Septal development varies, both cycles may be present up to 2/3R
Secondary septa		Present up to 1/4R	Usually incomplete to absent
Distally radial corallites		Tubo-nariform; towards the base, appressed tubular, sometimes walls extended by prostrate development	Tubo-nariform; towards the base, appressed tubular, sometimes walls extended by rostrate development
Coenosteum			
Texture	Consists of rows of laterally flattened or forked spinules, spongy between corallites	Reticulate	Reticulate
Radial corallites		Dense arrangement of laterally flattened or forked spinules	Dense arrangement of laterally flattened or forked spinules
Intercorallite areas		Spinules less densely arranged	Spinules less densely arranged
Other systematic information and remarks			
Similarity to other species	Have similar radial corallites and a coenosteum with <i>A. clathrata</i> but can differ by growth form. <i>Acropora scale</i> may be confused with <i>A. divaricata</i> but is readily distinguished by having radial corallites of two sizes, the larger having a tubular form.	Very similar to <i>Acropora solitariyensis</i> , distinguished mainly by growth form	Superficially does not resemble any other species. Closest affinities are with <i>A. divaricata</i>
Synotype information	–	Synotype of <i>Acropora stoddarti</i> Pilai & Scheer, 1976 is a flattened colony, growing on a wreck	Looks like a flattened form of <i>A. divaricata</i> , with branches sometimes forming a solid plate
Growth form variation	Wide range of skeletal variation within single biotopes, seldom develops well-defined, environment-related ecomorphs. One exception is sometimes found in coralla growing on soft substrates, or in turbid water where branchlets become flattened and the colony prostrate (viz. <i>A. stoddarti</i> Pilai & Scheer, 1976). In extreme cases, branchlets become fused into thin plates. Some skeletal developments (e.g. various types of corallite wall thickening and the development of naked branchlets) appear to be commonly associated with particular populations rather than particular environments.		Varies greatly in thickness of branches, can appear quite delicate or very sturdy
Continued			

	Acropora divaricata Veron and Wallace, 1984 ²³	Wallace, 1999 ²²	Acropora solitaryensis Veron and Wallace, 1984 ²³	Wallace, 1999 ²²
References				
Distribution			Abundant at specific locations but rare elsewhere. Divisible into five geographic subspecies, widely separated spatially and environmentally	Very common species in the Indian Ocean, Indonesia, and South China Sea. Surprisingly rare on the Great Barrier Reef proper as reported in Veron & Wallace, 1984
Geographic subspecies			Indicates five geographic subspecies, needing experimental verification to confirm as a single species unit	

Table 1. Identification criteria based on morphological characters used for distinguishing *Acropora solitaryensis* and *A. divaricata*. Due to the high resemblance of morphological characters that often complicate in-situ underwater identification of *Acropora solitaryensis* and *A. divaricata*, we conducted a comparative table of specific corallum characteristics, including branch pattern, size, and arrangement, to clarify the distinguishing features and similarities between these two species as referenced by Veron and Wallace (1984)²³, Wallace (1999)²².

conservation of corals is a top priority, planning for it can be confusing and overwhelming due to diverse species composition. With 1698 coral species in the order *Scleractinia*¹³ distributed from the tropics to high-latitude non-reefal communities¹⁴, working toward their protection is very difficult as they are morphologically plastic and challenging to identify genetically due to the lack of efficient molecular markers^{15,16}. Nevertheless, recent studies on coral taxonomy using integrative approaches (morphology, reproduction, and molecular) have gradually advanced our understanding of coral species^{17–21}.

The most dominant shallow water group, genus *Acropora*, with approximately 400 nominal species being abundant in tropical and subtropical reefs and high-latitude non-reefal communities in the three ocean provinces, represents a typical showcase for demonstrating integrative approaches to understanding coral taxonomy^{14,22}. Traditional methods for describing species that include the use of morphological characteristics such as growth form, corallite, and corallum structure^{22,23}, have not been effective in delineating species within *Acropora*, as its morphological traits are often unstable and subject to variation, either intraspecifically or interspecifically²⁴. For instance, skeletal characteristics such as size and shape of corallites can differ dramatically due to genetics, environmental factors²⁵, or even the location of corallites within the same colony^{14,22}. *Acropora* has been divided into 14 “species groups”²³ based on skeletal morphology to assist in classification and subsequent research. Nineteen Indo-Pacific and one Caribbean species group within the genus have been recognized²². Nevertheless, only 122 of approximately 400 nominal species are considered valid in the latest revision of the genus²⁶, and the phylogenetic implications of *Acropora* species groups remain unclear^{20,21,27–29}.

Inferring *Acropora* species phylogeny using conventional single-locus markers has shown incongruence patterns of mitochondrial and nuclear gene trees since the late 20th Century^{24,30–33}. This has been widely interpreted as evidence supporting either ongoing hybridization among coral species^{34,35}, or incomplete lineage sorting due to recent diversification of species groups as well as in species with large effective population sizes³⁶. In addition, the incorrect identification of specimens, which is highly likely in morphologically diverse groups such as *Acropora*, could also result in polyphyletic patterns observed in gene trees^{37,38}. Nevertheless, cryptic lineages of *Acropora* morphospecies complexes that have a broad geographic distribution in the Indo-Pacific region have recently been identified by multi-locus (microsatellites) and single-nucleotide polymorphism (SNP) genetic data in combination with the genotypic cluster species definition^{20,21,28,29,39–42}. Sequence data from 12 genomic regions have been used to clarify that *A. hyacinthus* collections from the Indo-Pacific region comprise at least four cryptic lineages³⁹. Two of the *A. hyacinthus* lineages have an unusual distributional pattern in East Asia, with one dominating marginal locations in Japan and Taiwan and the other dominating reefs of the Ryukyu Archipelago, Japan⁴⁰. Using microsatellites and single nucleotide polymorphisms (SNPs) derived from 2b-RAD sequencing, one lineage of *A. hyacinthus* identified in temperate Japan shows distinct bottleneck pressures, including higher clonality, increased linkage disequilibrium, and lower genetic diversity compared to subtropical populations^{41,42}. Combining morphological examination, genetic data of conventional single-locus markers, SNPs derived from the ultraconserved elements (UCEs) of hexacorallian genomes^{27,43}, and breeding trials successfully delineate distinct species boundaries among *A. bifurcata*, *A. cytherea*, and *A. hyacinthus*²⁸. The application of UCEs to examine species phylogeny in the *A. tenuis* clade by Cowman et al.²⁷ show this clade contains over 11 distinct lineages, only four of which correspond to then-accepted species based on morphological and geographical evidence, and allow the description of two new species, *A. rongi* and *A. tenuissima*²⁰. Population structure and principal component analyses with SNPs (> 60,000) indicate that *A. cf. bifurcata*, *A. cf. cytherea*, *A. cf. hyacinthus*, and *A. cf. subulata* are genetically distinct and do not show signs of introgression²¹. These findings collectively indicate that *Acropora* spp. diversity is higher than currently recognized, and widespread nominal species may represent multiple distinct species with restricted geographical distributions. To address this uncertainty, we employ provisional qualifiers (cf. = confer, aff. = affinis) in species names, as this approach reflects tentative identifications while awaiting further taxonomic confirmation.

In this study, we apply molecular phylogenetic and morphological approaches to delineate species boundaries for *Acropora* aff. *divaricata*⁴⁴ and *A. cf. solitaryensis*²³ collected from coral ecosystems in East Asia. Based on morphology, both species were previously categorized into the *divaricata* species group^{14,22}. This species group shares similar morphological characters, such as nariform with round or dimidiate openings of radial corallite, and determinate growth form with central to side-attached point of origin²². The holotype of *A. aff. divaricata* was described by Dana in 1846, with its type locality in Fiji. Its growth form is distinguished by nariform radial corallites with large, open calices and a reticulate coenosteum, despite variations in the density and arrangement of spinules (Table 1). At the colony level, *A. aff. divaricata* exhibits an open caespitose-corymbose branching pattern, forming branching colonies with tapering branches that can curve and anastomose to create a network within the colony²². This species also demonstrates different ecomorphs, as morphological variation within the species is extensive, including differences in branch dimensions, branching patterns, the development of corallites and branchlets, although environment-specific forms are generally not well-defined²³. *Acropora solitaryensis* is a relatively newly described species²³, similar in growth form with respect to branching patterns, corallite, and corallum structures to *A. divaricata*, but with a tendency to fuse into solid plates along basal branches^{22,23,45–47}. *Acropora solitaryensis* is abundant in high-latitude coral ecosystems, but also in the low-latitude Flinders Reef (Moreton Bay), Middleton Reef, and Solitary Islands in Australia. However, specimens of *A. solitaryensis* have also been reported and collected from the tropical Murray Reef, Martha Ridgeway Reef, and Palm Islands in the Great Barrier Reef²³. As a result of its unusual geographic distribution and morphological variability, it has been suggested that *A. solitaryensis* might be readily divisible into five geographic subspecies that are widely separated spatially and environmentally²³. On the other hand, its morphological plasticity also results in sympatric and continuous occurrences of colony morphs, including arborescent (AR), solid plate (PL), and intermediate (IM) forms, mainly in high-latitude coral ecosystems^{14,22,46–48}.

Both *A. divaricata* and *A. solitaryensis* have broad geographic distributions in the Pacific and Indian Oceans, with the former extending more to the Red Sea and the Persian/ Arabian Gulf^{14,22,49,50}. While²² confirms the

occurrence of *A. solitaryensis* in the central and west Indian Ocean¹⁴, they also confine its distribution to Sumatra and Indonesia in the east Indian Ocean. Both species are recorded from the island chain of East Asia, including Taiwan, Ryukyus Archipelago, and mainland Japan, with *A. divaricata* more in tropical and subtropical coral reefs and *A. solitaryensis* distributed further into high-latitude non-reefal coral ecosystems^{14,22,46,48,51}. Molecular phylogeny and cross-fertilization experiments have been used to examine the relationships among three morphs, namely arborescent (*A. solitaryensis_AR*), intermediate (*A. solitaryensis_IM*), and solid plate (*A. solitaryensis_PL*), of *A. solitaryensis* in the high-latitude non-reefal region in Japan⁴⁷ (Table S4). Their results show that *A. solitaryensis_AR* is distinct from *A. solitaryensis_PL*, suggesting no gene flow among the morphs. In their cross-fertilization experiments, gametic compatibility between *A. solitaryensis_AR* and *A. solitaryensis_PL* was extremely low, suggesting pre-zygotic isolation of these morphs. They conclude that *A. solitaryensis_AR* and *A. solitaryensis_IM* are variations of *A. solitaryensis*, whereas *A. solitaryensis_PL* may be an undescribed species. Interestingly, *A. solitaryensis_AR* and *A. solitaryensis_IM* form a monophyletic group in the molecular phylogenetic trees, with samples of *A. divaricata* collected from the subtropical islands Ishigaki and Miyako of the Ryukyus Archipelago⁴⁷. In contrast, applying morphometric, molecular phylogenetic, and cross-fertilization experiments to examine the cryptic boundary between two morphs of *A. divaricata*, “*A. divaricata_slender*” and “*A. divaricata_robust*,” in the central Ryukyus (Table S4), they show that although inter-morphotype gamete compatibility was high in the year of overlapping spawning seasons for these two distinct morphotypes, population genetics analyses and molecular phylogenetic analysis show that they are genetically distinct and rarely hybridize⁵². Their molecular phylogenetic tree of the mitochondrial control region grouped their “*A. divaricata_slender*” and the *A. solitaryensis_AR* into the clade of *A. divaricata*. On the other hand, their “*A. divaricata_robust*” grouped with *A. solitaryensis_PL*⁴⁷ from the high-latitude non-reefal region in Japan^{47,52}.

We hypothesize that the different growth forms of these two *Acropora* species collected from different geographical localities in the island groups of East Asia might represent two distinct lineages of the *A. divaricata* species group, one being *A. aff. divaricata* and the other *A. cf. solitaryensis*. To test this hypothesis, we collected *A. cf. solitaryensis* from the holotype locality in the north Solitary Island, Australia, and extended the sampling of both species to the waters off Taiwan, the largest continental island in East Asia. Taiwan has distinct tropical reef development to its southeast, whereas subtropical non-reefal coral communities exist to the northeast of its main island and Penghu Archipelago in the Taiwan Strait⁵³, and at high-latitude coral communities in Shikoku, Japan⁵⁴. By applying multi-locus molecular phylogenetic and morphological analyses, we confirm the species status of *A. aff. divaricata* and *A. cf. solitaryensis* in the East Asian island chain. While both species have sympatric occurrences in the subtropical reefs of the Ryukyus Archipelago and high-latitude non-reefal coral communities at mainland Japan, they have discrete distributions following a boundary separating tropical coral reefs and subtropical non-reefal coral communities in Taiwan.

Results

DNA sequence variation of molecular markers

Acropora samples ($n=124$) collected from Taiwan, Japan, and Australia were sequenced for *mtCR*, *MC*, *exon4706*, and *PMCA*. Published *mtCR* ($n=59$)^{24,47,52} and *MC* ($n=12$)^{47,55,56} DNA sequences were downloaded from DDBJ and GenBank. In total, 111 *mtCR*, 112 *MC*, 108 *exon4706*, and 108 *PMCA* sequences were utilized in phylogenetic analyses (Table 2). The aligned *mtCR* produced 80 bp of variable sites, but only 47.5% (48 bp) were phylogenetically informative sites. In contrast, the three markers derived from the nuclear genome provided high proportions of phylogenetically informative sites, ranging from 75.8% in *PMCA* to 81.6% in *MC* (Table 2, Fig. 1).

Molecular phylogenetic inferences and species delimitation

Our phylogenetic trees are based on *mtCR* from *Acropora* species from tropical reefs and subtropical non-reefal coral communities in Taiwan, subtropical coral reefs (Ryukyus), high-latitude coral communities (Shikoku, Japan), and non-reefal coral communities (Solitary Island, Australia) (Fig. 2A; Fig. S1-A). To help determine the taxonomic identity of our specimens, we included *A. divaricata* AY026432³¹ for reference in our dataset. Phylogenetic analyses were conducted to evaluate genetic similarity and assist in identifying the species of our specimens. Three major clades, namely *A. divaricata* (clade I), *A. solitaryensis* (clade II), and *A. japonica/tumida* (clade III), are supported by high ML bootstrapping and Bayesian inferences. Clade I is

Marker	Genome	Taxa	L (bp)	AL	VS	PI
Control region	Mitochondrial	111	778–989	742	80	38
Mini-collagen	Nuclear	112	462–508	210	49	40
4706	Nuclear	108	413–461	401	5	4
PMCA	Nuclear	108	542–608	487	33	25
Nuclear combined	4706-PMCA-mini collagen	108	1078–1097	1100	89	68

Table 2. Overview of genetic markers, genomic locations, and sequence characteristics. L = sequence length before alignment; AL = sequence length after alignment; VS = variable sites; PI = parsimony informative sites. The table summarizes the genetic markers used in this study, detailing their genomic locations, number of taxa analyzed for each marker, sequence length before alignment (L), sequence length after alignment (AL), number of variable sites (VS), and number of parsimony-informative sites (PI).

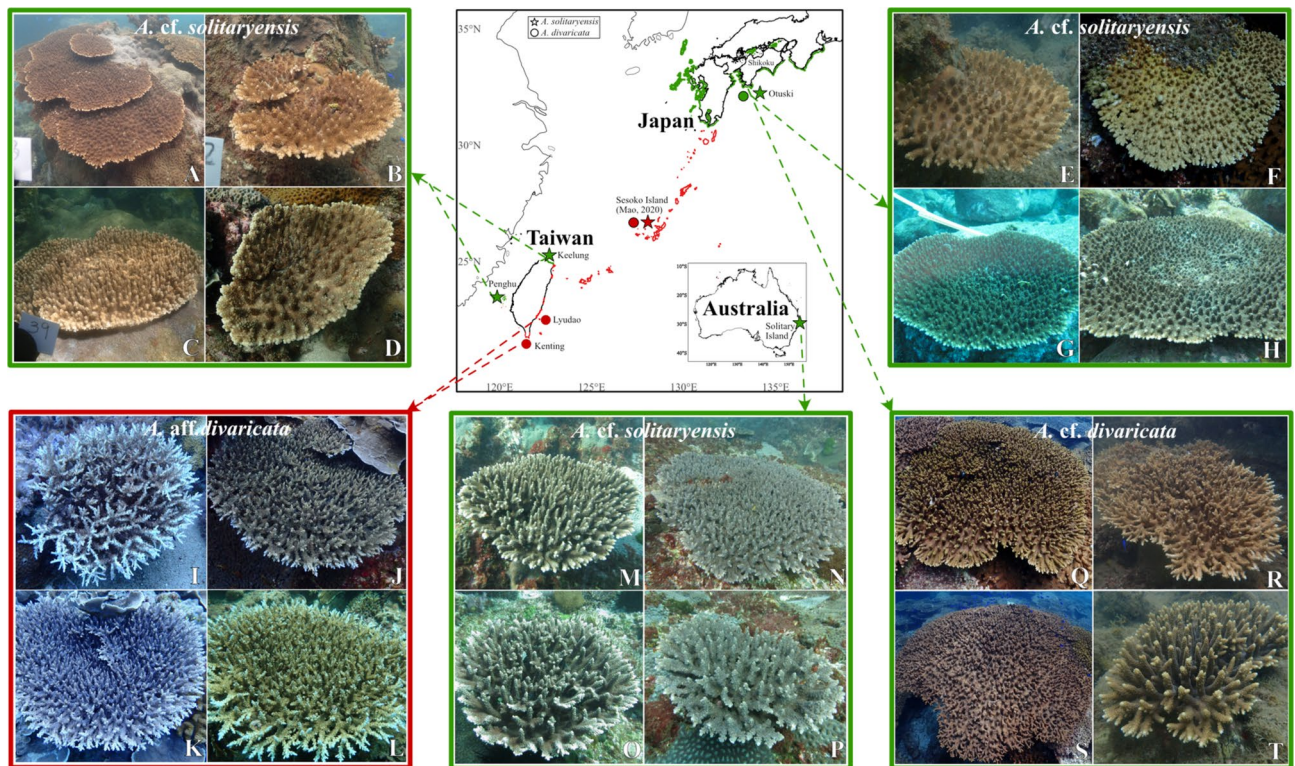


Fig. 1. Map of sampling localities and geographical distribution of identified species in tropical coral reefs (red) and non-reefal coral communities (green). *Acropora cf. solitaryensis* is predominantly found in non-reefal coral communities, specifically in northern Taiwan, Kochi Prefecture in Japan, and Solitary Island in Australia. Notably, it is also found in the tropical reef of Okinawa⁵². Conversely, *A. aff. divaricata* is located in tropical coral reef environments in southern Taiwan (Lyudao and Kenting) and Okinawa⁵², and non-reefal coral communities in Otuski (Kochi Prefecture, Shikoku).

composed of *mtCR* sequences from tropical reefs (Kenting and Green Island) in Taiwan, the “slender” form of *A. divaricata* (AdivSlender) from subtropical reefs of Ryukyus, Japan⁵², and the “arborescent” form of *A. solitaryensis* (Asolar) and *A. pruinosa* from high-latitude coral communities in Otuski, Shikoku, Japan⁴⁷. Clade II contains *mtCR* sequences from subtropical non-reefal coral communities (Keelung and Penghu) in Taiwan, the “robust” form of *A. divaricata* (AdivRobust) from subtropical reefs of Ryukyus, and the “solid plate” form of *A. solitaryensis* (AsolPL) from high-latitude coral communities in Otuski, Shikoku, Japan. Two *A. cf. solitaryensis* (5010, 5015) collected from Solitary Island, Australia, are grouped in clade II. The other two from Australia (5028, 5083) and seven from high-latitude Japan show a paraphyletic relationship with the three major clades (Fig. 2A); however, later analyses using nuclear genes support their grouping in clade II (Fig. 2B, C). Clade III is consistently composed of *A. japonica* and *A. tumida*.

Phylogenetic inferences based on nuclear genes support the relationship of three major clades (Fig. 2B,C; Fig. S1-B). The *MC* tree shows that clade I contains sequences of “Asolar”⁴⁷ samples from tropical reefs at Green Island and Kenting, Taiwan, and high-latitude coral communities in Otuski, Shikoku, Japan. Clade II, on the other hand, contains sequences of “AsolPL”⁴⁷ samples from subtropical non-reefal coral communities in Penghu and Keelung, Taiwan, and high-latitude coral communities in Otuski, Shikoku, Japan. The four *A. cf. solitaryensis* collected from Solitary Island are grouped within clade II. Clade III is sister to the monophyletic group of clades I and II (Fig. 2B). The tree generated by the combination of nuclear genes, *MC*, *exon4706*, and *PMCA*, shows a similar topology to the *MC* tree, with increasing ML bootstrapping and Bayesian support at the major nodes of the three clades (Fig. 2C).

Species delimitation analysis by DELINEATE⁵⁷ identified three major clades congruent with previously constructed phylogenetic trees (Fig. S3). The first clade corresponds to *A. aff. divaricata*, forming a cohesive and well-supported lineage across diverse localities (e.g., tropical reefs in Taiwan and non-reefal Japan). The second clade, *A. cf. solitaryensis*, includes the topotype locality (AU) as well as other populations (e.g., non-reefal Taiwan and Japan), indicating a clear evolutionary separation from the other clades. The third clade comprises *A. cf. tumida* and related taxa, including *A. cf. glauca* and *A. cf. japonica*, suggesting possible cryptic diversity or unrecognized species within this lineage.

Morphological differences between *A. aff. divaricata* and *A. cf. solitaryensis*

Our observations show various skeletal structures, including corallites, coenosteum, and spinules in *A. aff. divaricata* (Fig. 3A-C) and *A. cf. solitaryensis* (Fig. 3D-F). However, these descriptive variations are not variable

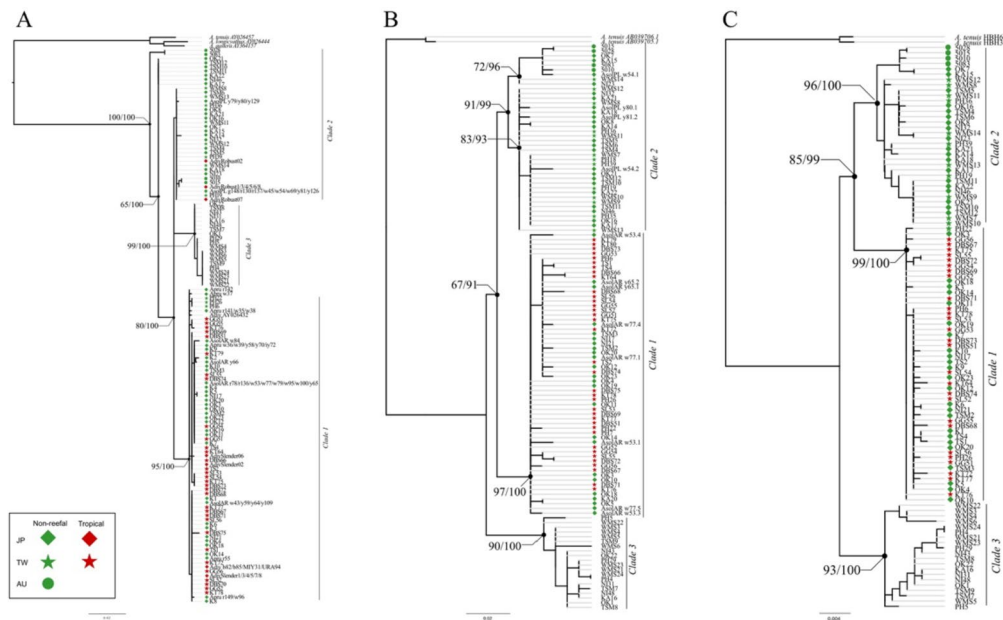


Fig. 2. Phylogenetic trees constructed using genetic data from our dataset and external sources^{47,52} for *Acropora* corals. These trees include (A) the mitochondrial control region (mtCR), (B) mini-collagen intron (MC), and (C) a selection of nuclear sequences (4706, PMCA, and mini-collagen). Branch base values indicate the percentages of trees from a total of 1000 replicate bootstrap maximum likelihood (ML) and Bayesian posterior probability analyses, in which corresponding taxa are grouped together. Branch lengths are proportional to the number of nucleotide substitutions per site, as the scale bar demonstrates. Specimens used in these analyses are from various locales across Taiwan (indicated by stars), Japan (indicated by diamonds), and Australia (indicated by circles), and from habitats categorized into tropical reefs (red) and non-reefal coral communities (green).

enough to distinguish between the two species (Fig. 3). The axial corallite of both species shares similar diameters ranging from 2.3 to 3.0 mm, calice diameters between 0.7 and 1.1 mm, and incomplete primary septa cycles with 1/2R to 1/4R (Fig. 3). The radial corallite is tubular on branch tips, with tubo-nariform to nariform and sub-immersed shapes on basal branches (Fig. 3). The coenosteum is costate in form, with spinules densely arranged between intercorallite regions (Fig. 3). In contrast, *A. aff. divaricata* and *A. cf. solitaryensis* can be distinguished by colony growth form (Fig. 1). *Acropora cf. solitaryensis* grows dominantly in the solid plate (PL) form, with colonies having anastomosed lower branches developing into flat basal plates, complemented by upright short branchlets (Fig. 1, A-D; E-H; M-P). Interestingly, juvenile colonies in the PL form show an additional characteristic: a semi-fused plate with an elongated, anastomosing, and upwardly curving branching pattern (Fig. 1, M, O, P). *Acropora aff. divaricata*, on the other hand, dominantly has an arborescent (AR) form that is distinctively characterized by an open caespitose-corymbose structure, with tapering branches and bowl/bracket-shaped colonies either centrally or laterally attached. The AR form exhibits stacked tables with spaced, anastomosing, and upwardly curving branchlets, which form an intricate network within the colony (Fig. 1, I-L; Q-T). A notable differentiation in some AR specimens from Lyudao (Fig. 1K) and Shikoku (Fig. 1Q, R, S) is the flattening of branchlets, leading the colony into a prostrate form and eventually fusing into thin plates (Fig. 1Q, R, S).

Overall branch widths (5 mm below axial corallites) and outer axial corallite diameters are significantly larger in *A. cf. solitaryensis* than in *A. aff. divaricata* (Fig. 4A, B; branch width, *A. divaricata*: 4.767 ± 1.196 mm, *A. solitaryensis*: 5.650 ± 1.046 mm, Tukey's HSD, $p < 0.001$; outer diameter of axial corallites, *A. aff. divaricata*: 1.833 ± 0.362 mm, *A. cf. solitaryensis*: 2.029 ± 0.318 mm, Wilcoxon signed rank test, $p < 0.001$; mean \pm SD), suggesting that *A. aff. divaricata* and *A. cf. solitaryensis* are morphometrically distinct. Intraspecific variations also occur in both the branch width and outer diameter of axial corallites in both species collected from Taiwan and Japan. In pairwise comparisons (Fig. S2), *A. aff. divaricata* in Taiwan has smaller branch widths (4.585 ± 1.176 mm) and smaller axial corallite outer diameters (1.732 ± 0.287 mm) than those from Japan (branch width: 5.525 ± 0.971 mm, Tukey's HSD, $p < 0.001$; corallite diameter: 2.290 ± 0.308 mm, Wilcoxon signed rank test, $p < 0.001$). In contrast, there are no differences in *A. cf. solitaryensis* branch widths collected from Japan and Taiwan (Japan: 5.793 ± 0.930 mm; Taiwan: 5.515 ± 1.150 mm, Tukey's HSD, $p > 0.05$) or in axial corallite outer diameters (Japan: 2.049 ± 0.323 mm; Taiwan: 2.003 ± 0.314 mm Wilcoxon signed rank test, $p > 0.05$).

Factorial Analysis of Mixed Data (FAMD)⁵⁸ was conducted using eight morphological characteristics (Table S3) for the examined specimens of *A. aff. divaricata* and *A. cf. solitaryensis* available for skeletal measurements (Table S1). The first five dimensions explained 84.04% of the total variance, with the first two dimensions capturing the largest proportions (Dim.1: 31.82%, Dim.2: 22.50%). The first dimension (Dim.1) was primarily influenced by axial_corallite_diameter (21.6%), branch_width (21.5%), and radial_corallite_openings (19.4%),

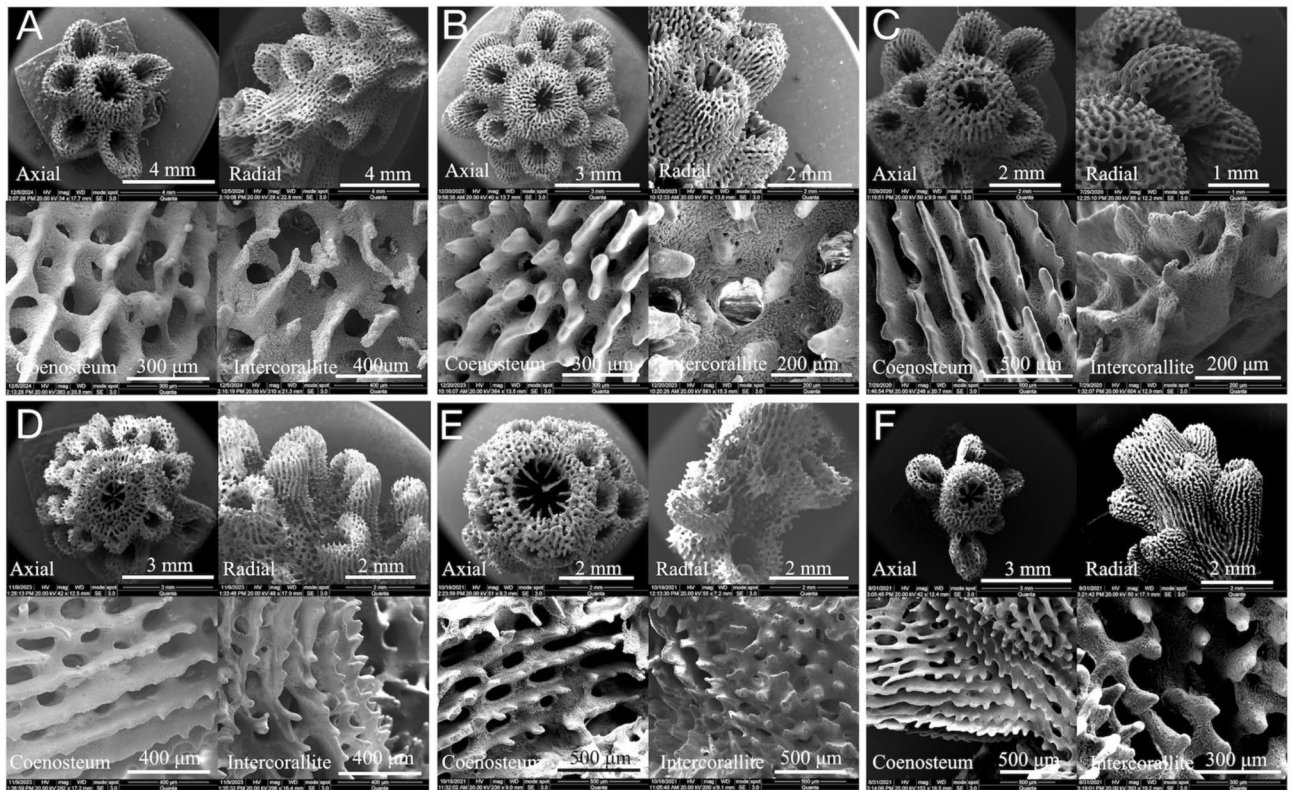


Fig. 3. Six images, each with four photographs, are arranged in a 2×2 grid. Each set represents a different specimen, with individual images highlighting specific morphological features observed under SEM in this study. Top left, axial corallite; top right, radial corallite; lower left, coenosteum; lower right, spinules between intercorallite. Specimens: *Acropora solitaryensis* from (A) Solitary Island, Australia; (B) Kawashijima, Japan; and (C) Keelung, Taiwan; and *Acropora divaricata* from (D) Nishidomari, Japan; (E) Kawashijima, Japan; and (F) Kenting, Taiwan.

separating populations along a gradient reflecting variation in axial corallite diameter and branch width (Fig. 4C). The second dimension (Dim.2) was largely influenced by growthForm (25.1%) and branch_width contributing (23.9%), with additional contributions from radial_crowding (20.3%) differentiating populations based on growth form and branching complexity.

The FAMD plot revealed a clear separation along the first two principal dimensions between the two focal species, *A. aff. divaricata* (red) and *A. cf. solitaryensis* (blue), as well as distinct clustering patterns associated with species and populations (Fig. 4C). The first dimension (Dim.1) effectively separated the samples from reefal and non-reefal environments, while the second dimension (Dim.2) differentiated the two species, *A. aff. divaricata* and *A. cf. solitaryensis*. Along Dim.1, reefal populations clustered towards negative axis, while non-reefal populations were positioned toward higher axis. Along Dim.2, *A. aff. divaricata* occupied positive axis, whereas *A. cf. solitaryensis* aligned with negative axis. *Acropora cf. solitaryensis* populations from non-reefal environments consistently clustered within quadrant 4 despite their greater dispersion, while *A. aff. divaricata*, occurring in both reefal and non-reefal habitats, displayed morphological traits in non-reefal settings that closely resembled those of *A. cf. solitaryensis* and differed significantly from its reefal counterparts, suggesting that environmental settings in non-reefal habitats may strongly influence coral morphology.

Discussion

Our study utilizes multi-locus phylogenetic approaches and morphometric measurements of skeletal structures to demonstrate that the different growth forms of *Acropora cf. solitaryensis* are distinct species in East Asian coral ecosystems. Those with arborescent or intermediate growth morphotypes, identified as *Acropora aff. divaricata* based on the literature, have a distribution range from tropical reefs in southeastern Taiwan to high-latitude temperate non-reefal coral communities in Shikoku, Japan. The solid plate morphotype, clustering with *A. cf. solitaryensis* collected from the holotype locality at Solitary Island, Australia, is distributed mainly in the subtropical non-reefal coral communities of the Penghu Islands, northern Taiwan, and Shikoku, Japan. The distinct distribution pattern of *A. aff. divaricata* and *A. cf. solitaryensis* found in this study highlights the urgent need to reconsider (1) biogeographic sampling when examining the taxonomy and systematics of *Acropora*, (2) the influence of the Kuroshio Current on the biogeographic patterns of corals, and (3) cautious interpretation of poleward migration and range expansion of corals in East Asia.

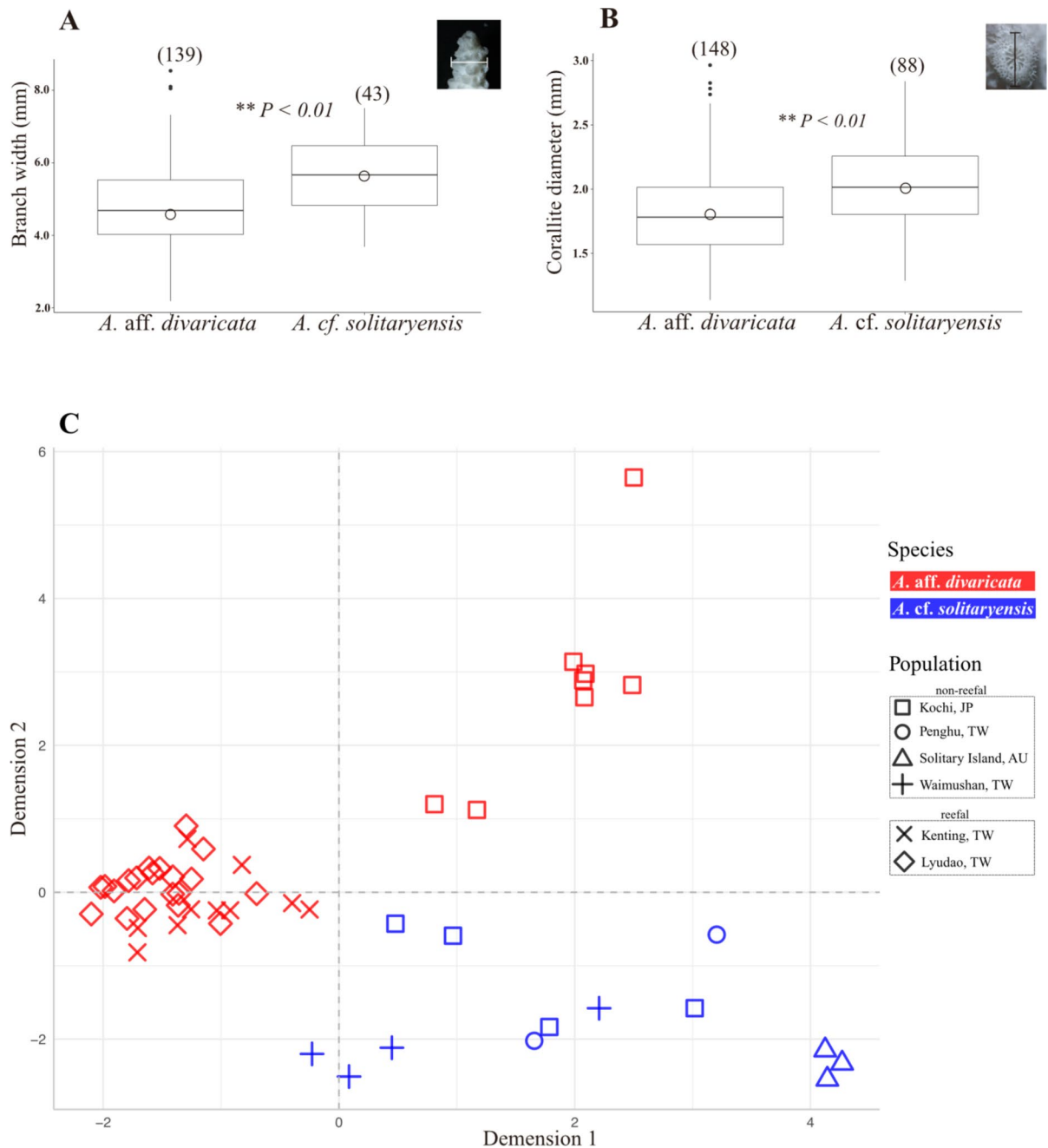


Fig. 4. Morphological differences: (A) branch width measured 5 mm below the axial corallites, and (B) corallite diameters of *A. aff. divaricata* and *A. cf. solitaryensis* collected from Japan and Taiwan. Box-and-whisker plots display the median (bold horizontal line), mean (red circle), interquartile range (box), range (whiskers), and outliers (dots). (C) Factor analysis of mixed data (FAMD) based on nine skeletal morphological characters, with each point representing an individual measurement from Taiwan, Japan, and Australia. FAMD successfully distinguishes *A. cf. solitaryensis* and *A. aff. divaricata*, as well as populations from tropical reefs and non-reefal coral communities.

Skeletal structures, including colony growth forms and corallite structures, are important traits for species identification and taxonomy in the genus *Acropora*²². It has been suggested that morphological variation among biogeographic locations and habitats and ambiguity of taxonomic characters make the delineation of species extremely difficult; therefore, morphotypes (or types) are used to describe the variants within species^{40,47,52}. In the case of *A. aff. divaricata* and *A. cf. solitaryensis*, extending biogeographic sampling of morphotypes helps clarify the morphological variation within and between species in high-latitude Japan and Taiwan. Based on molecular phylogeny and morphological measurements, *A. aff. divaricata* is diagnosed as arborescent, with stacked tables and anastomosing, upwardly curving branchlets that show intricate networks within colonies in the populations of tropical (Taiwan) and subtropical reefs (Ryukyus). In non-reefal coral communities (Shikoku), the branchlets

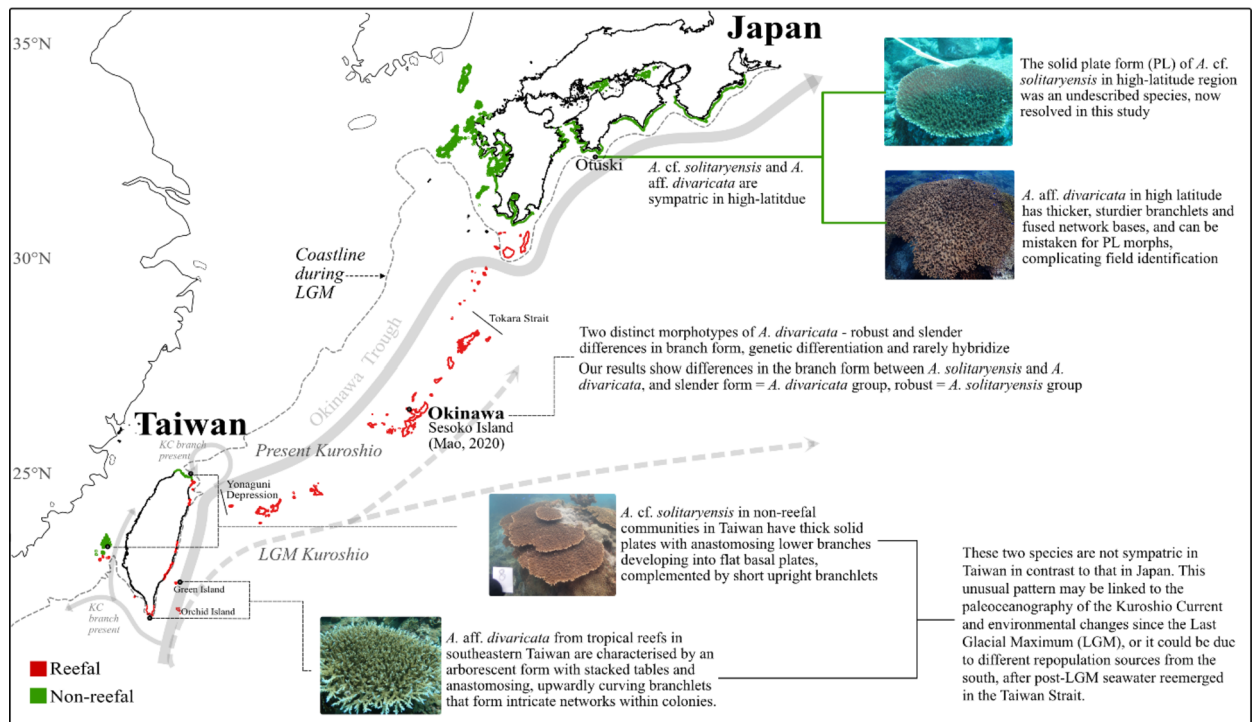


Fig. 5. Present and past (LGM) routes of the Kuroshio Current and the distribution of studied species, *Acropora cf. solitaryensis* and *Acropora aff. divaricata*. Red and green lines indicate reefal and non-reefal coral communities, respectively. The map illustrates the geographic range of these species across Taiwan and Japan, highlighting distinct morphological and ecological characteristics. The influence of the Kuroshio Current and the historical coastline during the Last Glacial Maximum (LGM) provide insights into the distribution patterns and population dynamics of these species. Representative morphotypes are shown, emphasizing the differences between the arborescent form of *A. aff. divaricata* and solid plate form of *A. cf. solitaryensis*, with their habitats.

of *A. aff. divaricata* colonies become thicker and sturdier, and their network bases become fused in comparison to reefal counterparts. This is a characteristic of corals adapted to harsher environmental conditions in the higher latitudes such as colder water temperatures and lower light levels⁵⁹. Adaptations to harsh environments are also seen in *A. cf. solitaryensis* collected from non-reefal coral communities in Taiwan and Shikoku, where colonies consistently have thick solid plates with anastomosing lower branches developing into flat basal plates, complemented by short upright branchlets. Interestingly, juvenile *A. cf. solitaryensis* show an additional semi-fused plate with an elongated, anastomosing, and upwardly curving branching pattern (IM form) that can be confused with sympatric *A. aff. divaricata* during field surveys and sample collections^{47,48,60–62}. This confusion is enhanced by the fact that the holotype of *A. cf. solitaryensis* described from Solitary Island^{22,23} is an IM form, leading⁴⁷ to the hypothesis that *A. solitaryensis_IM* and *A. solitaryensis_AR* are *A. solitaryensis* and *A. solitaryensis_PL* is likely an undescribed species in the non-reef region of Japan. Although the *A. cf. solitaryensis* topotypes collected from Solitary Island are IM morphotypes, molecular phylogeny shows them grouping with *A. solitaryensis_PL* (Fig. 2), thus rejecting the hypothesis proposed by⁴⁷.

In addition, the slender and robust morphotypes of *A. divaricata* in the subtropical Ryukyus are unambiguously assigned to different clades⁵². Their slender form is assigned together with AY026432 (*A. divaricata*) and *A. solitaryensis_AR*, whereas their robust form is assigned to *A. solitaryensis_PL*, based on mtCR phylogeny and STRUCTURE analyses, respectively⁵². Several lines of evidence suggest that slender and robust morphotypes of *A. divaricata* are likely distinct species. Firstly, branch sizes and axial diameters are significantly different. Secondly, the two morphotypes are reproductively isolated. Reproductive isolation is also observed in *A. solitaryensis_AR* and *A. solitaryensis_PL* in high-latitude Japan⁴⁷, indicating that pre-mating and postzygotic isolation mechanisms operate effectively in maintaining species boundaries, as seen in other sympatric *Acropora* species^{21,28,63–66}. Additional surveys, collections, and examinations of NGS markers of both morphotypes throughout the Ryukyus Archipelago are currently underway to confirm their affiliations with East Asian *A. aff. divaricata* and *A. cf. solitaryensis*.

Our study shows that both *A. aff. divaricata* and *A. cf. solitaryensis* are sympatric in subtropical reefs (Ryukyus) and the high-latitude non-reefal region (Shikoku) in Japan, but have a segregated distribution around the waters of Taiwan (Fig. 5). *Acropora aff. divaricata* is found in the tropical reefs of southeastern coast and islets in Taiwan, and *A. cf. solitaryensis* is restricted to the non-reefal communities along the northeastern coast, islets, and Penghu Archipelago in the Taiwan Strait. This unusual pattern might be related to the paleoceanography of the Kuroshio Current (KC) and environmental changes since the last glacial maximum (LGM, 20,000 yrs. BP) that have shaped the coral phylogeography in East Asia⁶⁵. The KC passes through Orchid Island and Green

Island off the east coast of Taiwan, across the Yonaguni Depression via the East Taiwan Channel into the East China Sea, and follows the edge of the continental shelf in the Okinawa Trough with a deep break between the ECS continental slope and the Ryukyu Archipelago (Fig. 5). It flows along the western part of the Okinawa Trough, and leaves the continental slope via the Tokara Strait, reaching the southern island of Japan at ~31°N (reviewed in⁵³). During the LGM, the sea level dropped 100–120 m, obstructing the KC from entering the Okinawa Trough⁶⁷, resulting in the KC flowing westward at a lower latitude than today^{68,69}. SST around the Japanese mainland was 5–6 °C lower than at present, which might have hindered reef development at the higher latitude. Fossil records have shown that coral reefs retreated from their current locations at southern Kyushu near Tanegashima to the southern Ryukyus near Miyazakijima-Ishigakijima (reviewed in Ref.⁶⁷). During the same period, the non-reefal regions of Taiwan that include the Penghu Archipelago and most of the north and northeast coast of Taiwan Island were exposed to air and remained part of the Asian landmass⁷⁰. The southern Ryukyus, therefore, likely served as a refugium for corals (and other reef organisms) that included *A. aff. divaricata* and *A. cf. solitaryensis* during the LGM in East Asia. After the LGM, the KC resumed its current position, temperatures gradually increased and peaked 2–3 °C higher at ~6,000 yrs. BP, and sea-level rose 2–3 m higher than at present in Japan and Taiwan^{70,71}. Sea surface temperature warming during this period enabled coral populations to extend their ranges northward to reach the Japanese mainland, as did non-reefal coral communities to northern Taiwan and the Penghu Archipelago. Fossil records indicate that tropical fauna, including hermatypic corals, were distributed at higher latitudes (~35°N) 6,000 yrs. BP^{72,73}. Similar fossil coral and crustose coralline algae (CCA) assemblages are recorded along the coast of Taoyuan City, northwest Taiwan (~25°N) 7500–6000 yrs. BP^{70,74}. After global cooling occurred 4000 yrs. BP, also known as the Little Ice Age in the Northern Hemisphere (LIANH⁷⁵), reef development in Japan retreated from higher latitudes to its current position near Tanegashima⁶⁷ (30°N). Along the coast of Taoyuan City, Taiwan, most corals could not survive lower temperatures, freshwater intrusion, and highly sedimented surroundings during the LIANH. CCA became the dominant reef-builders and have continuously constructed unprecedented algal reefs unto the present^{74,76,77}. During this period, the benthic communities of high-latitude coasts in Japan were dominated by kelp (*Ecklonia* spp.) and fucoid seaweed (*Sargassum* spp.) until the early 21st Century, being gradually replaced by corals and CCA due to SST rising caused by climate change⁷⁸. An examination of museum collections since the 1930s suggests that three *Acropora* species including *A. solitaryensis* have responded to rising SST by range expansions into the high-latitude non-reefal region in Japan⁷⁹. Similar speculation of the influence of KC on coral distribution along East Asia is also made for *A. hyacinthus*⁴⁰.

The alternative hypothesis explaining the segregated distribution pattern of *A. aff. divaricata* and *A. cf. solitaryensis* in Taiwan is that the sources for repopulating these species differ after post-GLM seawater reemerged in the Taiwan Strait. During the GLM, *A. aff. divaricata* could have maintained its occurrence on the coast and islets of southeast Taiwan in the Pacific. *Acropora cf. solitaryensis*, on the other hand, needed to repopulate the Penghu Archipelago in the Taiwan Strait and northern Taiwan from sources further south, such as Dongsha Atoll in the South China Sea⁸⁰, which served as a southern refugium for corals and reef-associated organisms during the LGM. Future surveys, collections, and phylogeographic genomic analyses of both species in the South China Sea are needed to test these two hypotheses.

Taxonomy plays an important role in conservation planning for coral species and theoretical inferences such as poleward range expansion. Our finding that both *A. cf. solitaryensis* and *A. aff. divaricata* co-occur at the high latitudes of Japan highlight the need to revisit the scenario of tropical coral poleward migration and/or range expansion in East Asia⁷⁹. Based on our literature reviews and examination of museum collections, we suggest that *Acropora* species, including *A. solitaryensis*, *A. hyacinthus*, and *A. muricata*, have expanded from their previous northern distribution limits within the East Asian region (Tokara and Tanegashima) to higher latitudes in Japan since the 1930s, with the speed of these expansions reaching up to 14 km/yr. However, readers need to take note of ever-changing taxonomic analyses of corals due to their morphological and genetic complexities within and among locations. Recent studies have demonstrated that nominal species within *Acropora* and other coral taxa possess greater diversity than previously recognized^{20,27,43}. This suggests that species once considered pandemic across the Indo-Pacific may comprise multiple distinct, geographically restricted species²⁰. Consequently, *Acropora* spp. may be far more diverse than currently understood, potentially encompassing several distinct species within what are presently classified as single taxa. In this study, the two species *A. cf. solitaryensis* and *A. aff. divaricata* both exhibit notable taxonomic complexities. *A. solitaryensis* described by Veron and Wallace in 1983 may comprise up to five geographic subspecies. Its trans-equatorial distribution and significant morphological variability, combined with the limitations of current genetic markers, highlight its unresolved taxonomy. Although we included topotypes of *A. cf. solitaryensis* in our study, it is likely that the taxonomic status of this species will be revised in the future. Similarly, *A. divaricata*, originally described by Dana in 1846 from its type locality in Fiji, faces comparable taxonomic ambiguity^{23,52}. Moreover, its type locality is approximately 7,700 km from Taiwan, resulting in substantial geographical separation. This distance, along with observed morphological differences, suggests that the populations identified as *A. aff. divaricata* in this study may represent geographically separated but genetically distinct species. These findings underscore the urgent need to revisit the taxonomy, systematics, and biogeography of *Acropora* spp. more broadly. Enhanced genomic approaches are essential to accurately delineate species boundaries and understand the true diversity within this ecologically significant genus^{20,27–29,42,43}. Moreover, the collaborative “Project Phoenix” (<https://coralprojectphoenix.org>) is working towards resolving issues related to coral taxonomy across the oceans (For example, see²⁸). Our study demonstrates that *A. cf. solitaryensis* in high latitudes is indeed mixed with *A. aff. divaricata*, questioning not only which of the two species is expanding its range but also risking mixing expansion speed calculations for these two species. Nevertheless, clarification of the species status of *A. aff. divaricata* and *A. cf. solitaryensis* allows us to establish a diagnostic framework for differentiating them in the field and lab, and

provides a good species pair for reexamining the hypothesis of poleward migration and range expansion of *Acropora* spp. in East Asia in response to rising SST caused by climate change.

Methods

Coral sampling and identification

Sampling for *Acropora* cf. *solitaryensis* was conducted by SCUBA diving primarily in Taiwan and Japan between 2013 and 2023 (Fig. 1 and Table S1). Additionally, samples were collected in 2016 from Solitary Island, Australia (Permit No. P12/0050–1.0), the locality from where the holotype of *A.* cf. *solitaryensis* was described²³. This was to confirm the phylogenetic status of *A.* cf. *solitaryensis* in the northern hemisphere. The identification of coral species followed^{22,23}. Due to the high resemblance of morphological characters that easily confuses in-situ underwater identifications of *A.* cf. *solitaryensis* and *A.* aff. *divaricata* (Table 1), we targeted colonies fitting the descriptions of corallum characters, including branching pattern, size, and arrangement. Additional *Acropora* species, *A.* cf. *japonica*, *A.* cf. *pruinosa*, and *A.* cf. *tumida*, which occur sympatrically with *A.* cf. *solitaryensis*⁴⁸, were also sampled from the non-reefal coral communities of Penghu Island (Permit No. 03751) and Keelung (Permit No. 1090225216), Taiwan (Permit No. 11258843900), and Otsuki, Shikoku, Japan (Permit No. 768). The outgroup, *A.* aff. *striata*, was collected from the tropical reef in Kenting National Park, southern Taiwan. Growth form, branch pattern, and a close-up of radial corallites of each sampled colony were photographed with an Olympus TG-6 camera. Samples containing at least three branches of coral colonies were chiseled off, returned to the shore, and preserved in 80% EtOH before cutting off small pieces (5 cm long) for DNA extraction. The remaining samples were bleached in 10% sodium hypochlorite solution for morphological examination. The bleached skeletons were deposited in the Biodiversity Research Museum, Academia Sinica, with voucher numbers listed in Table S1. Formal identification of coral samples was done by Chaolun Allen Chen in Taiwan, Chaolun Allen Chen and Takuma Mezaki in Japan, and Andrew H. Baird in Australia.

Molecular phylogenetic analysis and species delimitation

Total genomic DNA was extracted using NautiaZ Tissue DNA Extraction Mini Kit (Nautia Gene, Taiwan) following the manufacturer's protocol. Four genetic markers, the mitochondrial control region⁴⁷ (*mtCR*), intron region of the nuclear mini-collagen (*MC*)⁸¹ gene, nuclear gene Exon 4706 (*4706*)³⁹, and exon plasma membrane calcium-transporting ATPase (*PMCA*)³⁹, were subjected to polymerase chain (PCR) reactions to obtain DNA sequences for phylogenetic analyses. A total volume of 25 μ l PCR recipe contained 0.5 μ l of genomic DNA template, 0.5 μ l of each primer (10 μ M), 12.5 μ l of Taq DNA Polymerase Master Mix RED (Ampliqon, Denmark), and 10.5 μ l of ddH₂O. PCR primers, temperature settings, and cycle numbers are listed in Table S2.

PCR products were Sanger sequenced for forward and reverse strands by Genomics Biotech (Taipei, Taiwan). Forward and reverse strands of DNA sequences were assembled and trimmed by Geneious Prime 2023.2.1 (<https://www.geneious.com>). DNA sequences of all markers obtained in this study were submitted to the NCBI Genbank under accession numbers listed in Table S1. DNA sequences were aligned using Clustal Omega v 1.2.3⁸² before phylogenetic construction.

Phylogenetic tree constructions were based on (1) *mtCR*, (2) *MC*, and (3) a combination of three nuclear genes (*4706*, *PMCA*, and *MC*). Firstly, we compiled our data with the previously published *mtCR* and *MC* DNA sequences of other *Acropora* species to visualize the overall phylogenetic relationships^{24,56}. This preliminary analysis allowed us to visualize the overall phylogeny of our samples, including *A.* aff. *divaricata*, *A.* cf. *solitaryensis*, *A.* cf. *japonica*, and *A.* cf. *tumida*, alongside other non-*divaricata*-*solitaryensis* species. As expected, the phylogenetic trees (Fig. S1) revealed topological incongruence for some non-*divaricata*-*solitaryensis* species, with their distribution across the tree suggesting non-monophyletic relationships, which complicated the interpretation of the relationship between *A.* aff. *divaricata* and *A.* cf. *solitaryensis*. Based on these initial results, we focused our subsequent phylogenetic analyses on the reduced dataset containing only *A.* aff. *divaricata*, *A.* cf. *solitaryensis*, *A.* cf. *japonica*, and *A.* cf. *tumida* for further phylogenetic analyses with the early-spawning clade of *A.* aff. *striata*, *A.* *longicyathus*, and *A.* *austera*, as outgroups^{24,47,52,56}. The analyses employed maximum likelihood (ML, 1000 bootstrap replicates) and Bayesian inferences (ngen = 1,100,000, samplefreq = 200, burnin = 500, nruns = 2) with convergence assessed using Effective Sample Size (ESS > 200) and Potential Scale Reduction Factor (PSRF ~ 1.0), indicating sufficient sampling and convergence of the Markov chain. Nucleotide substitution models were selected using Modeltest-NG v0.1.7⁸³. Substitution models, information on gamma distribution, and proportion of invariable sites for the ML inference and models selected for Bayesian inference are listed in Table S2. ML trees were constructed using RAXMLGUI V2.0 v8⁸⁴, and Bayesian inferences were executed in BEAST2 v2.7.7⁸⁵. Final trees were imported into FigTree V.1.4.4 (<http://tree.bio.ed.ac.uk/software/figtree/>) and Affinity Designer V1.0.8 to refine tree shapes, labels, and tags.

We tested different species boundaries hypotheses in DELINEATE⁵⁷. The analysis was performed based on the online program manual. The dataset was partitioned into hypothetical populations using the "A10" analysis implemented in BPP v4.3^{86,87}. Individuals in this study are lumped as candidate population units based on sampling locations. Guide Tree for population delimitation was generated by StarBeast2⁸⁸ (single strick clock model, HKY + G, ngen = 500,000,000, samplefreq = 500,000, burn-in = 250, n-runs = 4) in BEAST v. 2.7.7⁸⁵ with convergence assessed using Effective Sample Size (ESS > 200), indicating sufficient sampling and convergence of the Markov chain. The final guide tree was summarized by SumTrees using maximum clade credibility tree (MCCT) topology. BP&P v4.3 was implemented again with the guide tree to run under A10 mode to delimit true population units. Distinct population lineages under a posterior probability threshold of 0.95 were used, and the original population label with collapsed multiple candidate population lineages used as traits for generating ultrametric phylogeny of population lineages by StarBeast2 (single strick clock model, HKY + G, ngen = 400,000,000, samplefreq = 400,000, burn-in = 250, n-runs = 6). SumTrees was implemented to select the Maximum Clade Credibility Tree (MCCT) as the summary topology for DELINEATE. For the constrain

table, the lineages of *A. cf. solitaryensis* from Solitary Island were set as the constrained lineage, with others being unconstrained lineages for DELINEATE analysis to explore all possible partitions that vary in the species assignments of these populations. DELINEATE was run with the MCCT tree and constraints table based on all partitions contributing over 0.99 (-P 0.99) of the probabilities to generate the final tree with species delimitation.

Morphological variation analyses

Morphological characters were obtained through photographs of bleached skeleton samples. Coral branches and branching patterns were photographed using a Nikon Coolpix P6000 digital camera. Corallites and septa were captured with Olympus Stereomicroscope System SZ51 with an OLYMPUS DP72 CCD camera. All images were processed using cellSens Standard 1.6 imaging software (Evident Corporation, Japan). Synapticular rings and coenosteia were visualized and documented using scanning electron microscopy (FEI Quanta 200 equipped with a Quorum PP2000TR FEI system). Quantitative data such as axial corallite branch diameter, branch width, and axial corallite length were measured by ImageJ. Descriptive (qualitative data) growth forms and skeletal characteristics of coral samples, including coral branching patterns (radial_crowding, growth_form, branching_orders, branch_width_contributing), growth form, corallites (axial_corallite_diameter, branch_width, axial_corallite_length, radial_corallite_shape, radial_corallite_openings), septa, and coenosteia, were used in *A. cf. solitaryensis* and *A. aff. divaricata* species identification and FAMD analysis (Table S3)^{14,22,23,89}. We compared branch widths and axial corallites by the methods modified by Furukawa et al.^{21,52} to determine whether skeletal differences exist among samples collected from different geographical locations. Branch widths (5 mm below the axial corallites) and outer diameters of axial corallites, which are specific to species level (*A. aff. divaricata* and *A. cf. solitaryensis*) and geographic level (Japan and Taiwan), were measured. The Shapiro-Wilk normality test⁹⁰ showed that branch widths conformed to a normal distribution; thus, ANOVA and Tukey's HSD were applied⁹¹ to examine the differences in branch widths across different localities (Japan and Taiwan). In contrast, Shapiro-Wilk normality testing showed that the outer diameter of axial corallites had a high W value (0.98354) but low P-value (<0.05). We applied the Wilcoxon signed rank test⁹² to examine the difference in corallite diameter between *A. aff. divaricata* and *A. cf. solitaryensis*. All analyses were done in R-package (version 4.3.2). To explore the multivariate relationships among mixed-type variables (quantitative and qualitative, Table S3), we conducted a Factorial Analysis of Mixed Data (FAMD)⁵⁸ using R (version 4.3.2). The preprocessing steps included averaging multiple data points from each colony to ensure representative values for analysis. Categorical variables were converted to factors as required by the FactoMineR package⁹³, with the number of dimensions determined based on eigenvalue contributions and cumulative variance explained. Key visualizations, including individual maps, variable contribution plots, and biplots, were created using factoextra and ggplot2. The viridis package was applied to enhance graphical clarity with perceptually uniform and interpretable color gradients.

Data availability

Sequence data supporting the findings of this study have been deposited in the National Center for Biotechnology Information (NCBI) database, with accession codes provided in the supplementary information. Voucher specimens, along with their corresponding voucher numbers, are detailed in the Materials and Methods section and supplementary files.

Received: 30 August 2024; Accepted: 10 February 2025

Published online: 21 March 2025

References

- Hughes, T. P. et al. Coral reefs in the anthropocene. *Nature* **546**, 82–90 (2017).
- Intergovernmental Panel on Climate Change (IPCC). *Global Warming of 1.5°C: IPCC Special Report on Impacts of Global Warming of 1.5°C above pre-industrial Levels in Context of Strengthening Response to Climate Change, Sustainable Development, and Efforts to Eradicate Poverty* (Cambridge University Press, 2022). <https://doi.org/10.1017/9781009157940>.
- Hoegh-Guldberg, O., Poloczanska, E. S., Skirving, W. & Dove, S. Coral reef ecosystems under climate change and ocean acidification. *Front. Mar. Sci.* **4**, 158 (2017).
- Hughes, T. P. et al. Global warming transforms coral reef assemblages. *Nature* **556**, 492–496 (2018).
- Zande, R. M. et al. Paradise lost: end-of-century warming and acidification under business-as-usual emissions have severe consequences for symbiotic corals. *Glob. Chang Biol.* **26**, 2203–2219 (2020).
- Beyer, H. L. et al. Risk-sensitive planning for conserving coral reefs under rapid climate change. *Conserv. Lett.* **11** (2018).
- Hoegh-Guldberg, O., Kennedy, E. V., Beyer, H. L., McClennen, C. & Possingham H. P. securing a long-term future for coral reefs. *Trends Ecol. Evol.* **33**, 936–944 (2018).
- Anthony, K. R. N. et al. Interventions to help coral reefs under global change—A complex decision challenge. *PLoS One* **15**, e0236399 (2020).
- Chauka, L. J. & Nyangoko, B. P. Climate change impacts outweigh conservation efforts in coral reefs that are highly exposed to thermal stresses in Zanzibar, Tanzania. *Ocean. Coast Manag.* **238**, 106575 (2023).
- Hilmi, N. et al. The pressures and opportunities for coral reef preservation and restoration in the Maldives. *Front. Environ. Econ.* **2**, 1110214 (2023).
- Gove, J. M. et al. Coral reefs benefit from reduced land–sea impacts under ocean warming. *Nature* **621**, 536–542 (2023).
- Battaglia, F. M. Blue planet law, the ecology of our economic and technological world. *Sustain. Dev. Goals Ser.* 121–130. https://doi.org/10.1007/978-3-031-24888-7_10 (2023).
- Bernot, J. et al. World Register of Marine Species (WoRMS) (2024).
- Veron, J. E. N. Corals of the World, 1–3 (Australian Institute of Marine Science and CRR, 2000).
- Fukami, H. Short review: molecular phylogenetic analyses of reef corals. *Galaxea J. Coral Reef. Stud.* **10**, 47–55 (2008).
- Fukami, H., Tachikawa, H., Suzuki, G., Nagata, S. & Sugihara, K. Current status and problems with the identification and taxonomy of zooxanthellate scleractinian corals in Japan. *J. Jpn. Coral Reef. Soc.* **12**, 17–31 (2010).
- Kitahara, M. V., Fukami, H., Benzoni, F. & Huang, D. The Cnidaria, past, present and future, 41–59 https://doi.org/10.1007/978-3-319-31305-4_4 (2016).

18. Arrigoni, R. et al. An integrated morpho-molecular approach to delineate species boundaries of *Millepora* from the Red Sea. *Coral Reefs*. **37**, 967–984 (2018).
19. Terraneo, T. I., Benzoni, F., Baird, A. H., Arrigoni, R. & Berumen, M. L. Morphology and molecules reveal two new species of *Porites* (Scleractinia, Poritidae) from the Red Sea and the Gulf of Aden. *Syst. Biodivers.* **17**, 491–508 (2019).
20. Bridge, T. C. L. et al. A *tenuis* relationship: traditional taxonomy obscures systematics and biogeography of the '*Acropora tenuis*' (Scleractinia: Acroporidae) species complex. *Zoöl J. Linn. Soc. zlad062* <https://doi.org/10.1093/zoolinnean/zlad062> (2023).
21. Furukawa, M. et al. Integrative taxonomic analyses reveal that rapid genetic divergence drives *Acropora* speciation. *Mol. Phylogenet. Evol.* **195**, 108063 (2024).
22. Wallace, C. Staghorn corals of the world. 10.1071/9780643101388 (1999).
23. Veron, J. E. N., John, E. N. & Wallace, C. C. Scleractinia of eastern Australia. Part V. Family Acroporidae. *Scleractinia East. Australia Part. V* **6**, 1–485 (1984).
24. Fukami, H., Niimura, A., Nakamori, T. & Iryu, Y. Species composition and mitochondrial molecular phylogeny of *Acropora* corals in Funakoshi, Amami-Oshima Island, Japan: a proposal for its new taxonomic grouping. *Galaxea J. Coral Reef. Stud.* **23**, 17–35 (2021).
25. Todd, P. A. Morphological plasticity in scleractinian corals. *Biol. Rev.* **83**, 315–337 (2008).
26. Wallace, C., Done, B. & Muir, P. Revision and catalogue of worldwide staghorn corals *Acropora* and *Isopora* (Scleractinia: Acroporidae) in the Museum of Tropical Queensland. *Mem. Qld. Mus. - Nat.* **57**, 1–255 (2012).
27. Cowman, P. F. et al. An enhanced target-enrichment bait set for Hexacorallia provides phylogenomic resolution of the staghorn corals (Acroporidae) and close relatives. *Mol. Phylogenet. Evol.* **153**, 106944 (2020).
28. Ramirez-Portilla, C. et al. Solving the coral species delimitation conundrum. *Syst. Biol.* **71**, 461–475 (2021).
29. Ramirez-Portilla, C. et al. Quantitative three-dimensional morphological analysis supports species discrimination in complex-shaped and taxonomically challenging corals. *Front. Mar. Sci.* **9**, 955582 (2022).
30. Odorico, D. M. & Miller, D. J. Variation in the ribosomal internal transcribed spacers and 5.8S rDNA among five species of *Acropora* (Cnidaria; Scleractinia): patterns of variation consistent with reticulate evolution. *Mol. Biol. Evol.* **14**, 465–473 (1997).
31. van Oppen, M. J. H., McDonald, B. J., Willis, B. & Miller, D. J. The evolutionary history of the coral genus *Acropora* (Scleractinia, Cnidaria) based on a mitochondrial and a nuclear marker: reticulation, incomplete lineage sorting, or morphological convergence? *Mol. Biol. Evol.* **18**, 1315–1329 (2001).
32. Márquez, L. M., Oppen, M. J. H. V., Willis, B. L., Reyes, A. & Miller, D. J. The highly cross-fertile coral species, *Acropora hyacinthus* and *Acropora cytherea*, constitute statistically distinguishable lineages. *Mol. Ecol.* **11**, 1339–1349 (2002).
33. Richards, Z. T., Berry, O. & van Oppen, M. J. H. Cryptic genetic divergence within threatened species of *Acropora* coral from the Indian and Pacific oceans. *Conserv. Genet.* **17**, 577–591 (2016).
34. Veron, J. E. N. *Corals in Space and Time: The Biogeography and Evolution of the Scleractinia* (Cornell University Press, 1995).
35. Willis, B. L., van Oppen, M. J. H., Miller, D. J., Vollmer, S. V. & Ayre, D. J. The role of hybridization in the evolution of reef corals. *Ecol. Evol. Syst.* **37**, 489–517 (2006).
36. Fukami, H., Omori, M. & Hatta, M. Phylogenetic relationships in the coral family acroporidae, reassessed by inference from mitochondrial genes. *Zoöl Sci.* **17**, 689–696 (2000).
37. Wolstenholme, J. K., Wallace, C. C. & Chen, C. A. Species boundaries within the *Acropora humilis* species group (Cnidaria; Scleractinia): a morphological and molecular interpretation of evolution. *Coral Reefs* **22**, 155–166 (2003).
38. Richards, Z. T., Miller, D. J. & Wallace, C. C. Molecular phylogenetics of geographically restricted *Acropora* species: implications for threatened species conservation. *Mol. Phylogenet. Evol.* **69**, 837–851 (2013).
39. Ladner, J. T. & Palumbi, S. R. Extensive sympatry, cryptic diversity and introgression throughout the geographic distribution of two coral species complexes. *Mol. Ecol.* **21**, 2224–2238 (2012).
40. Suzuki, G. et al. Genetic evidence of peripheral isolation and low diversity in marginal populations of the *Acropora hyacinthus* complex. *Coral Reefs*. **35**, 1419–1432 (2016).
41. Nakabayashi, A. et al. The potential role of temperate Japanese regions as refugia for the coral *Acropora hyacinthus* in the face of climate change. *Sci. Rep.* **9**, 1892 (2019).
42. Fifer, J. E., Yasuda, N., Yamakita, T., Bove, C. B. & Davies, S. W. Genetic divergence and range expansion in a western North Pacific coral. *Sci. Total Environ.* **813**, 152423 (2022).
43. Quattrini, A. M. et al. Universal target-enrichment baits for anthozoan (Cnidaria) phylogenomics: new approaches to long-standing problems. *Mol. Ecol. Resour.* **18**, 281–295 (2018).
44. Dana, J. D. Zoophytes. United States exploring expedition during the years 1838–1842 (1846).
45. Veron, J. E. N. (*John E. N. Hermatypic Corals of Japan* (Australian Institute of Marine Science, 1992).
46. Dai, C. & Horng, S. Scleractinia Fauna of Taiwan I. The Complex Group (National Taiwan University, 2009).
47. Suzuki, G. & Fukami, H. Evidence of genetic and reproductive isolation between two morphs of subtropical-dominant coral *Acropora solitariaensis* in the non-reef region of Japan. *Zoöl Sci.* **29**, 134–140 (2012).
48. Nishihira, M. & Veron, J. E. N. *Hermatypic Corals of Japan* (Kaiyusha, 1995).
49. Veron, J. E. N., (John, E. N., Marsh, M., Museum, W. A. & Loiset, L. *Hermatypic Corals of Western Australia: Records and Annotated Species List* (Western Australian Museum, 1988).
50. Veron, J. E. N. (John E. N. *A Biogeographic Database of Hermatypic Coral Species of the Central Indo-Pacific, Genera of the World* (Australian Institute of Marine Science, 1993).
51. Dai, C. & Cheng, Y. R. *Corals of Taiwan: Scleractinia Fauna* Vol. 1 (Owl Publishing House Co., LTD, 2020).
52. Furukawa, M., Ohki, S., Kitanobo, S., Fukami, H. & Morita, M. Differences in spawning time drive cryptic speciation in the coral *Acropora divaricata*. *Mar. Biol.* **167**, 163 (2020).
53. Kuo, C. Y. et al. Coral reefs of Eastern Asia under Anthropogenic impacts. *Coral Reefs World*, 7–35. https://doi.org/10.1007/978-3-031-27560-9_2 (2023).
54. Keshavmurthy, S., Mezaki, T., Reimer, J. D., Choi, K. S. & Chen, C. A. Coral reefs of Eastern Asia under anthropogenic impacts. *Coral Reefs World*, 53–71. https://doi.org/10.1007/978-3-031-27560-9_4 (2023).
55. Hatta, M. et al. Reproductive and genetic evidence for a reticulate evolutionary history of mass-spawning corals. *Mol. Biol. Evol.* **16**, 1607–1613 (1999).
56. Fukami, H., Omori, M., Shimoike, K., Hayashibara, T. & Hatta, M. Ecological and genetic aspects of reproductive isolation by different spawning times in *Acropora* corals. *Mar. Biol.* **142**, 679–684 (2003).
57. Sukumaran, J., Holder, M. T. & Knowles, L. L. Incorporating the speciation process into species delimitation. *PLoS Comput. Biol.* **17**, e1008924 (2021).
58. Pagès, J. Factorial analysis of mixed data. *J. Appl. Stat.* **52**, 93–111 (2004).
59. Chong, F. et al. High-latitude marginal reefs support fewer but bigger corals than their tropical counterparts. *Ecography* **2023** (2023).
60. Sugihara, K. et al. Zooxanthellate scleractinian corals of Tanegashima Island, 1–197 (2015).
61. Nomura, K. The illustrated zooxanthellate scleractinian corals of Kushimoto I REFERTINA. *Marine Pavilion* 1–56 (2016).
62. Nomura, K. et al. Revision of the zooxanthellate scleractinian corals in Kushimoto, Wakayama, Japan. *Mar. Pavilion* (2016).
63. Mrquez, L. M., van Oppen, M. J. H., Willis, B. L. & J. Miller, D. Sympatric populations of the highly cross-fertile coral species *Acropora hyacinthus* and *Acropora cytherea* are genetically distinct. *Proc. R. Soc. Lond. Ser. B Biol. Sci.* **269**, 1289–1294 (2002).

64. Wei, N. V. et al. Reproductive isolation among *Acropora* species (Scleractinia: Acroporidae) in a marginal coral assemblage. *Zool. Stud.* **51**, 85–92 (2012).
65. Ohki, S., Kowalski, R. K., Kitanobo, S. & Morita, M. Changes in spawning time led to the speciation of the broadcast spawning corals *Acropora digitifera* and the cryptic species *Acropora* sp. 1 with similar gamete recognition systems. *Coral Reefs*. **34**, 1189–1198 (2015).
66. Kitanobo, S., Isomura, N., Fukami, H., Iwao, K. & Morita, M. The reef-building coral *Acropora* conditionally hybridize under sperm limitation. *Biol. Lett.* **12**, 20160511 (2016).
67. Gallagher, S. J. et al. The Pliocene to recent history of the Kuroshio and Tsushima currents: a multi-proxy approach. *Prog Earth Planet. Sci.* **2**, 17 (2015).
68. Ujiie, H., Tanaka, Y. & Ono, T. Late quaternary paleoceanographic record from the middle Ryukyu Trench slope, northwest Pacific. *Mar. Micropaleontol.* **18**, 115–128 (1991).
69. Ujiie, Y., Ujiie, H., Taira, A., Nakamura, T. & Oguri, K. Spatial and temporal variability of surface water in the Kuroshio source region, Pacific Ocean, over the past 21,000 years: evidence from planktonic foraminifera. *Mar. Micropaleontol.* **49**, 335–364 (2004).
70. Dai, C., Wang, S. & Chang, J. *Handbook for Ecological Tours of Guanyin Algae Reef* (Liquefied Natural Gas Engineering Office, CPC Corporation, 2009).
71. Schöne, B. R. et al. Holocene seasonal environmental trends at Tokyo Bay, Japan, reconstructed from bivalve mollusk shells—implications for changes in the east Asian monsoon and latitudinal shifts of the Polar Front. *Quat Sci. Rev.* **23**, 1137–1150 (2004).
72. Hoshino, M. The absolute age of the Numa Coral reef, Chiba prefecture. *14 C-Age Quaternary Deposits Japan XXXVI*. **21**, 38–39 (1967).
73. Matsushima, Y. Shallow marine molluscan assemblages of postglacial period in the Japan islands—its historical and geographical changes induced by the environmental changes. *Bull. Kanagawa Prefectural Museum*. **15**, 37–109 (1984).
74. Liou, C. Y., Yang, S. Y. & Chen, C. A. Unprecedented calcareous algal reefs in northern Taiwan merit high conservation priority. *Coral Reefs* **36**, 1253–1253 (2017).
75. Chen, M. et al. Enhanced monsoon-driven upwelling in southeast Asia during the little ice age. *Paleoceanogr. Paleoclimatol.* **38** (2023).
76. Kuo, C. Y. et al. Lonely giant on the sand: unexpected massive Taiwanese coral, *Polycyathus chaishanensis* in the Danan algal reef demands a conservation focus. *Galaxea J. Coral Reef Stud.* **21**, 11–12 (2019).
77. Kuo, C. Y. et al. Demographic census confirms a stable population of the critically-endangered caryophyllid coral *Polycyathus chaishanensis* (Scleractinia; Caryophyllidae) in the Danan Algal Reef, Taiwan. *Sci. Rep.* **10**, 10585 (2020).
78. Serisawa, Y., Imoto, Z., Ishikawa, T. & Ohno, M. Decline of the *Ecklonia cava* population associated with increased seawater temperatures in Tosa Bay, southern Japan. *Fish. Sci.* **70**, 189–191 (2004).
79. Yamano, H., Sugihara, K. & Nomura, K. Rapid poleward range expansion of tropical reef corals in response to rising sea surface temperatures. *Geophys. Res. Lett.* **38** (2011).
80. Tkachenko, K. S., Soong, K. & Dongsha Atoll A potential thermal refuge for reef-building corals in the South China Sea. *Mar. Environ. Res.* **127**, 112–125 (2017).
81. Wang, W. et al. Isolation and characterization of a mini-collagen gene encoding a nematocyst capsule protein from a reef-building coral, *Acropora donei*. *Gene* **152**, 195–200 (1995).
82. Sievers, F. et al. Fast, scalable generation of high-quality protein multiple sequence alignments using Clustal Omega. *Mol. Syst. Biol.* **7**, 539–539 (2011).
83. Darriba, D. et al. ModelTest-NG: a new and scalable tool for the selection of DNA and protein evolutionary models. *Mol. Biol. Evol.* **37**, 291–294 (2020).
84. Edler, D., Klein, J., Antonelli, A. & Silvestro, D. raxmlGUI 2.0: a graphical interface and toolkit for phylogenetic analyses using RAxML. *Methods Ecol. Evol.* **12**, 373–377 (2021).
85. Bouckaert, R. et al. BEAST 2: a software platform for bayesian evolutionary analysis. *PLoS Comput. Biol.* **10**, e1003537 (2014).
86. Yang, Z. & Rannala, B. Unguided species delimitation using DNA sequence data from multiple loci. *Mol. Biol. Evol.* **31**, 3125–3135 (2014).
87. Flouri, T., Jiao, X., Rannala, B. & Yang, Z. Species tree inference with BPP using genomic sequences and the multispecies coalescent. *Mol. Biol. Evol.* **35**, 2585–2593 (2018).
88. Barido-Sottani, J. et al. Taming the BEAST—A community teaching material resource for BEAST 2. *Syst. Biol.* **67**, 170–174 (2018).
89. Wallace, C. C. & Dai, C. F. Scleractinia of Taiwan (IV): review of the coral genus *Acropora* from Taiwan. *Zool. Stud. Taipei* **36**, 288–324 (1997).
90. Royston, P. Approximating the Shapiro-Wilk W-test for non-normality. *Stat. Comput.* **2**, 117–119 (1992).
91. Tukey, J. Multiple comparisons. *J. Am. Stat. Assoc.* **48**, 624–625 (1953).
92. Trawiński, B., Smętek, M., Telec, Z. & Lasota, T. Nonparametric statistical analysis for multiple comparison of machine learning regression algorithms. *Int. J. Appl. Math. Comput. Sci.* **22**, 867–881 (2012).
93. Lê, S., Josse, J., Husson, F. & FactoMineR An R package for multivariate analysis. *J. Stat. Softw.* **25** (2008).

Acknowledgements

We thank members of the Coral Lab, Biodiversity Research Center, Academia Sinica (BRCAS), for support in field sampling, molecular technique, and analysis. We also extend our gratitude to Andrew H. Baird for providing the Australian specimen and permit, and Silvia Fontana for sample collection in Japan. This work was funded by NSTC 111-2740-M-001-004, AS-4010-PI, AS-100-TP2-A02-SUB, AS-TP-111-L03, AS-4010-PI, MOST 109-2621-B-001-002-MY2; all to CAC. The Postdoctoral Research Fellowship to SK is funded by the Ministry of Science and Technology, Taiwan. SWC is supported by the doctorate fellowship of the Taiwan International Graduate Program, Academia Sinica of Taiwan.

Author contributions

SWC - Sample processing, molecular and statistical analysis, wrote the manuscript with contributions from CAC and SK. CHC - Morphology, morphometry, and statistical analysis. DYT - Logistics, sampling, and statistical analysis. TM and SKu - Samples from Japan, morphology, and permits. HJH - Sampling logistics, permitting, and funding in Penghu. SK - Supervision, manuscript revision, and guidance. CAC - writing, conceived, and oversaw project development, overall logistics, and funding. All authors contributed to the final draft manuscript. All authors edited and approved the final version.

Declarations

Competing interests

The authors declare no competing interests.

Additional information

Supplementary Information The online version contains supplementary material available at <https://doi.org/10.1038/s41598-025-90051-x>.

Correspondence and requests for materials should be addressed to S.K. or C.A.C.

Reprints and permissions information is available at www.nature.com/reprints.

Publisher's note Springer Nature remains neutral with regard to jurisdictional claims in published maps and institutional affiliations.

Open Access This article is licensed under a Creative Commons Attribution-NonCommercial-NoDerivatives 4.0 International License, which permits any non-commercial use, sharing, distribution and reproduction in any medium or format, as long as you give appropriate credit to the original author(s) and the source, provide a link to the Creative Commons licence, and indicate if you modified the licensed material. You do not have permission under this licence to share adapted material derived from this article or parts of it. The images or other third party material in this article are included in the article's Creative Commons licence, unless indicated otherwise in a credit line to the material. If material is not included in the article's Creative Commons licence and your intended use is not permitted by statutory regulation or exceeds the permitted use, you will need to obtain permission directly from the copyright holder. To view a copy of this licence, visit <http://creativecommons.org/licenses/by-nc-nd/4.0/>.

© The Author(s) 2025